

Received March 23, 2018, accepted May 15, 2018, date of publication May 21, 2018, date of current version June 29, 2018.

Digital Object Identifier 10.1109/ACCESS.2018.2838590

# An Indoor Localization Method Based on AOA and PDOA Using Virtual Stations in Multipath and NLOS Environments for Passive UHF RFID

YONGTAO MA<sup>1</sup>, (Member, IEEE), BOBO WANG<sup>1</sup>, SHUYANG PEI<sup>1</sup>, YUNLEI ZHANG<sup>1</sup>, SHUAI ZHANG<sup>1</sup>, AND JIEXIAO YU<sup>2</sup>, (Member, IEEE)

<sup>1</sup>School of Microelectronics, Tianjin University, Tianjin 300072, China

<sup>2</sup>School of Electronics and Information Engineering, Tianjin University, Tianjin 300072, China

Corresponding author: Yongtao Ma (mayongtao@tju.edu.cn)

This work was supported in part by the Natural Science Foundation of China under Grant 61671318, Grant 61501322, and Grant 61401301, and in part by the Tianjin Research Program of Application Foundation and Advanced Technology under Grant 15JCQJNC41900.

**ABSTRACT** Ultra-high frequency radio frequency identification (UHF RFID) localization technique has been considered increasingly promising in indoor positioning systems. However, conventional localization algorithms are vulnerable in multipath and non-line of sight (NLOS) environments. To solve this problem, this paper presents an indoor localization method based on angle of arrival and phase difference of arrival (PDOA) using virtual stations for passive UHF RFID. We use the array antenna to distinguish multipath signals and choose the two strongest paths according to the received signal strength to perform localization. The angles of the two paths are obtained through the phase difference of the received signals at different array elements, and the distances of the two paths are estimated through PDOA measurement. After obtaining the angles and distances, we establish virtual stations to convert NLOS paths into LOS paths. The possible positions of the tag are calculated through virtual stations, angle, and distance information, which are derived from the two signal paths. Then, the weighted least squares combined with residual weighted algorithm are proposed to calculate real position of the tag. Simulation results demonstrate that our method achieves decimeter level accuracy and has higher precision than traditional algorithms.

**INDEX TERMS** AOA, PDOA, multipath, NLOS, UHF RFID, virtual stations.

## I. INTRODUCTION

Indoor localization has become exceedingly important in various applications [1]. At the same time, ultra-high frequency radio frequency identification (UHF RFID) technology is getting more and more consideration to be the optimal selection for indoor positioning systems because it is contactless, low cost and has high accuracy [2], [3].

Due to the complex signal propagations caused by walls, clapboard, ceiling and so on, the UHF RFID signals may suffer from reflections, refractions and diffractions. The accuracy of indoor localization will be affected by the phenomenon of non-line of sight (NLOS) and multipath arrivals seriously.

The methods of indoor localization include time of arrival (TOA) [4], time difference of arrival (TDOA) [5], received signal strength (RSS) [6], angle of arrival (AOA) [7]–[9],

phase difference of arrival (PDOA) [10], [11] and some combinations of these methods. However, TOA and TDOA are quite difficult to be implemented in UHF RFID systems because of its narrow bandwidth. The method based on RSS is sensitive to fading and multipath effects, so its accuracy is not very high. The accuracy of PDOA method is closely related to multipath effect and AOA method suffers from the effects of NLOS and multipath propagations.

To improve the accuracy of indoor localization, a robust algorithm named residual weighted multidimensional scaling (RWMDS) based on the multipath channel model is proposed in [10], whereas this algorithm cannot work well in NLOS environment. A new localization method based on joint iterative phase reconstruction and weighted localization algorithm with convex optimization has been proposed to fulfill high accuracy in NLOS environment using RFID signals in [12],

but the transmitted and received signals paths at the same reader may be different which may cause large errors. A RSS based algorithm that selects a special subset of array antennas to perform AOA estimations based on UHF RFID is proposed in paper [13], which needs multiple array antennas to estimate the transponder position. Yang *et al.* [14] attempt to improve localization precision of a passive RFID localization system by using sparsely distributed RFID tags. However, the localization precision is related to the distribution of RFID tags. A two-stage positioning approach is developed to improve position accuracy for tracking vehicles in NLOS propagation environments in [15], which needs LOS measurements to smooth the distance estimates. Liu *et al.* [14] propose a fine-grained backscatter positioning technique using the commercial off-the-shelf RFID products with detected phases. The method in [17] tries to identify the NLOS paths from a set of mixed LOS and NLOS measurements, which requires LOS involved. A new tracking filter that accepts orientation estimates as input is proposed to improve tracking accuracy in RFID tracking systems [18]. A novel stochastic localization algorithm called LOCUST is proposed [19], where functional dependency between pair wise received signal strength indicator (RSSI) cross correlation measured by a tag reader is used to infer the unknown location of the RFID tags, but this algorithm takes more computation time to increase localization accuracy. An item-level indoor localization with passive UHF RFID based on tag interaction analysis is presented in [20], which needs to measure localization of reference tags in advance.

In order to better mitigate the effects of NLOS and multipath on the accuracy of indoor localization, in this paper, we combine AOA with PDOA methods to implement an indoor localization method based on passive UHF RFID. From paper [21] and [22], we know that AOA estimation can be made only if the direction of the incoming signal is within the radiation pattern of main beam. Therefore, we can use the array antenna with narrow beamwidth to distinguish the multipath signals. The angles of the two paths are obtained through the phase difference of the received signals at different array elements.

For AOA estimation, classical algorithms are multiple signal classification (MUSIC) and estimation of signal parameters via rotational invariance techniques (ESPRIT) [23]. In indoor environment, multipath signals are highly correlated because of reflections. MUSIC method uses spatial smoothing as decorrelation technique. Instead of using MUSIC method, in this paper, we use an algorithm called method of direction estimation (MODE) [24] to perform the AOA estimation. Compared with MUSIC algorithm, MODE has a better performance for correlated or coherent sources. The distances of the two paths are estimated through PDOA measurement.

To mitigate the effect of NLOS path, we establish virtual stations to convert NLOS paths to LOS paths [25]. The possible positions of the tag are calculated through virtual stations, angle and distance information which are derived from the

two signal paths. WLS-RW algorithm is used to calculate the real position of the tag. To evaluate the performance of our proposed method, we derive the Cramér-Rao Lower Bounds (CRLB) of AOA and PDOA estimation respectively [26]–[28], and then calculate the CRLB of the localization error based on the WLS-RW algorithm.

The rest of this paper is organised as follows: the channel model of passive UHF RFID is introduced in Section II. Section III presents the proposed method. Location estimation algorithm and the CRLB is provided in section IV. Simulation analysis is given in Section V. Finally, Section VI provides a concluding summary.

## II. CHANNEL MODEL OF PASSIVE UHF RFID

### A. CHANNEL MODEL BASED ON RSS

According to the Friis Transmission Equation [29], in free space, for one direct path, the received signal power (or received signal strength, RSS) is:

$$P_R = P_T \left( \frac{\lambda}{4\pi d} \right)^2 \quad (1)$$

where  $P_T$  is the power of transmitted signal,  $d$  is the length of direct path,  $\lambda$  is the wavelength of signal.

The workflow of a passive RFID system is as follows: RFID reader transmits a modulated RF signal to a RFID tag which consists of an antenna with an integrated circuit chip. Then the chip receives power from the antenna. It modulates and responds the signal by varying its input impedance. We suppose that the uplink is identical to the downlink, and in clutter indoor environment, there must be some reflection paths, so the Friis equation can be modified as follows [30]:

$$P_R = P_T \frac{G_r^2 G_t^2 X^2 \xi^2 L_p^2}{\rho^2 \alpha^2} \quad (2)$$

where  $G_r$  is gain of the reader,  $G_t$  is gain of the tag,  $X$  is the polarization match factor,  $\xi$  is modulation factor of the tag,  $\alpha$  is the path loss exponent,  $\rho$  is compensation of the antenna gain, and  $L_p$  is the path loss:

$$L_p = \left( \frac{\lambda}{4\pi} \right)^2 \left| \frac{1}{d_0} e^{-jk d_0} + \sum_{i=1}^N \Gamma_i \frac{1}{d_i} e^{-jk d_i} \right|^2 \quad (3)$$

where  $k = 2\pi/\lambda$ ,  $d_0$  is the length of direct path,  $d_i$  is the length of the  $i$ th reflection path,  $N$  is the total number of reflection paths,  $\Gamma_i$  is polarization related reflection coefficient of the  $i$ th reflection path.

### B. CHANNEL MODEL BASED ON AOA

We suppose there are  $M$  elements in the array antenna, and  $K$  is the number of antenna elements and also is the number of the far field narrowband signal. We use  $s_i(t)$  to represent the signal source:

$$s_i(t) = u_i(t) e^{j(\omega_0 t + \varphi(t))} \quad i = 1, 2, \dots, K. \quad (4)$$

where  $u_i(t)$  is the amplitude of the signal,  $\omega_0$  is the angular frequency,  $\varphi(t)$  is the phase. After time delay  $\tau$ :

$$s_i(t - \tau) = u_i(t - \tau) e^{j(\omega_0(t - \tau) + \varphi(t - \tau))} \quad (5)$$

For far field narrowband signals:

$$\begin{cases} u_i(t) \approx u_i(t - \tau) \\ \varphi(t) \approx \varphi(t - \tau) \end{cases} \quad (6)$$

so, we can obtain:

$$s_i(t - \tau) \approx s_i(t)e^{-j\omega_0\tau} \quad (7)$$

At time  $t$ , the received signals are:

$$X(t) = AS(t) + e(t) \quad (8)$$

where

$$A = [a(\theta_1), a(\theta_2), \dots, a(\theta_K)]^T \quad (9)$$

$$a(\theta_i) = [e^{-j2\pi f \tau_{i1}}, \dots, e^{-j2\pi f \tau_{Mi}}]^T \quad (10)$$

$S(t) = [s_1(t), s_2(t), \dots, s_K(t)]^T$  is the vector of the signal waveform, and  $e(t) = [e_1(t), e_2(t), \dots, e_M(t)]^T$  is the vector of noise.

If the array is a Uniform Linear Array (ULA) and the reference element is at the original point, the time delay of the  $j$ th signal at the array element  $i$  is  $\tau_{ij} = x_i \sin(\theta_j)/c$ ,  $i = 1, 2, \dots, M, j = 1, 2, \dots, K$ , where  $x_i$  is the location if the  $i$ th array element,  $c$  is the propagation velocity of the electromagnetic wave in air.

### C. CHANNEL MODEL BASED ON PDOA

We use  $H(f)$  to represent the multipath channel response in frequency domain:

$$H(f) = \alpha_0 e^{-j2\pi f \tau_0} + \sum_{i=1}^N \alpha_i e^{-j2\pi f \tau_i} \quad (11)$$

where  $\alpha_0$  is the amplitude of direct path arriving at delay  $\tau_0$ ,  $\alpha_i$  is the amplitude of  $i$ th path arriving at delay  $\tau_i$ ,  $f$  is the frequency of signal. To obtain the phase of arrival signal, we can use the following equation:

$$\Delta\phi = \arctan\left(\frac{Im(H)}{Re(H)}\right) \quad (12)$$

where  $Im\{\cdot\}$  and  $Re\{\cdot\}$  are real part and imaginary part of a complex number respectively.

### III. THE PROPOSED METHOD

The base station (BS) is a ULA and the inter-element spacing is half wavelength with respect to the center frequency of UHF RFID. As shown in Fig. 1, the center of the BS is at the origin of the two-dimensional coordinate system and the ULA is arranged along the  $x$  axis. Because of the obstacle there may be no LOS path and we suppose that there are two NLOS paths.

The proposed method includes four steps:

- 1) Use the array antenna with narrow beamwidth to distinguish at least two signal paths and estimate the angle of arrivals;
- 2) Measure the length of two paths through PDOA method;

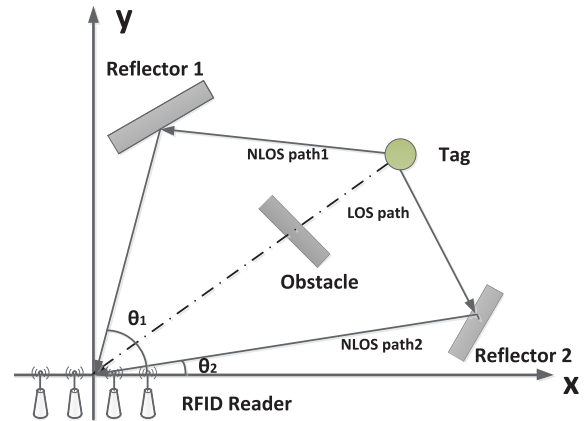


FIGURE 1. An indoor localization model in NLOS and multipath environments based on UHF RFID. There are two NLOS paths and there is no LOS path.

- 3) Establish virtual stations and find possible positions of the tag;
- 4) Calculate the location of the tag with WLS-RW algorithm.

#### A. AOA ESTIMATION

For AOA estimation, classical algorithms are MUSIC and ESPRIT. In indoor environment, multipath signals are highly correlated because of reflections. MUSIC method uses spatial smoothing as decorrelation technique. Instead of using MUSIC method with spatial smoothing, in this paper, we use an algorithm called method of MODE to perform the AOA estimation. Compared with MUSIC algorithm with spatial smoothing, MODE has a better performance for correlated and coherent sources.

The far-field region is defined by three conditions:

$$\begin{cases} d \gg \lambda \\ d \gg D \\ d > 2D^2/\lambda \end{cases} \quad (13)$$

where  $d$  is the observation distance,  $\lambda$  is the wavelength at the operation frequency and  $D$  is size of the antenna.

If the central frequency  $f_c$  of UHF RFID signal is 925MHz,  $\lambda = 0.32m$ , the antenna size  $D$  is about 0.5m, according to formula (13), if  $d$  is larger than 1.5m, we can approximately think the ULA is in the far-field region. In a far-field region, RFID signals can be regarded as plane-waves.

For a ULA, the beamwidth can be calculated through the following equation:

$$BW \approx \frac{51^\circ}{D\lambda} \quad (14)$$

where the antenna size  $D = (M - 1)\lambda/2$ ,  $M$  is the number of array element,  $\lambda$  is the wavelength at the operation frequency. When the angle between two signal paths is larger than beamwidth, array antenna can distinguish these two signals. Then we can use AOA estimation algorithms to calculate angles.

Suppose there are  $M$  identical antenna elements in the ULA and the distance between each element is half of the wavelength  $\lambda$ ; the number of the far-field narrowband signals is  $K$ ; at time  $t$ , the received signals at the  $m$ th array element can be expressed as:

$$h_m = \sum_{k=1}^K s_k(t) e^{-j2\pi f_c \tau_{mk}} + \omega_m \quad m = 1, 2, \dots, M. \quad (15)$$

where  $\omega_m$  is the zero-mean additive white Gaussian noise with variance  $\sigma^2$ ,  $\tau_{mk}$  is the propagation delay that a signal need to arrive at other array elements compared with the reference element.

Let the rightmost array element be the reference element:

$$\tau_{mk} = \lambda(m - 1) \cos(\theta_k) / 2c \quad (16)$$

where  $\theta_k$  is the angle between the  $k$ th signal and the positive  $x$  axis,  $\theta_k \in [0, \pi]$ ,  $c$  is the propagation velocity of electromagnetic wave in air.

Use a vector matrix  $H$  to represent the received signals at the  $M$  array elements:

$$H = [h_1, h_2, \dots, h_M]^T \quad (17)$$

The covariance matrix of  $H$  is :

$$R = E\{HH^H\} \quad (18)$$

where  $\{\cdot\}^H$  means conjugate transpose operation, and  $E\{\cdot\}$  is the expectation operator.

$R$  can be written as follows through eigenvalue decomposition:

$$R = U_s \Lambda_s (V_s)^H + U_n \Lambda_n (V_n)^H \quad (19)$$

where the columns of  $U_s \in \mathbb{C}^{M \times K}$  contain the signal subspace eigenvectors, the columns of  $U_n \in \mathbb{C}^{M \times (M-K)}$  contain the noise subspace eigenvectors, diagonal matrix  $\Lambda_s = \text{diag}\{\lambda_1, \lambda_2, \dots, \lambda_K\}$  contains  $K$  signal subspace eigenvalues, diagonal matrix  $\Lambda_n = \text{diag}\{\lambda_{K+1}, \lambda_{K+2}, \dots, \lambda_M\}$  contains  $(M - K)$  noise subspace eigenvalues.

Define a complex vector  $b$  [24]:

$$b = [b_0, b_1, \dots, b_K]^T \quad (20)$$

where  $\{b_i\}$  is defined by the following equation:

$$b_0 + b_1 z + \dots + b_K z^K = b_0 \prod_{k=1}^K (1 - e^{j\pi \cos(\theta_k)}) \quad (21)$$

where  $\omega_k = \pi \cos(\theta_k)$ . Since the polynomial on the left-hand side of equation (21) has all its zeroes on the unit circle, its coefficients  $\{b_i\}$  must satisfy conjugate symmetry constraint [31].

Let  $B \in \mathbb{C}^{M \times (M-K)}$  be a standard Toeplitz matrix [32]:

$$B^H = \begin{bmatrix} b_0 & \dots & b_K & & 0 \\ & \ddots & & \ddots & \\ 0 & & b_0 & \dots & b_K \end{bmatrix} \quad (22)$$

Define the loss function called  $\mathcal{F}(b)$ :

$$\mathcal{F}(b) = \text{tr}\{\mathcal{P}(b)U_s W(U_s)^H\} \quad (23)$$

where  $\text{tr}\{\cdot\}$  is the trace of a matrix. Suppose matrix  $B$  and matrix  $\Lambda_s$  are non-singular,  $\mathcal{P}(b) = B(B^H B)^{-1} B^H$ ,  $W = (\Lambda_s - \sigma^2 I)^2 \Lambda_s^{-1}$ ,  $\sigma^2$  is the estimated noise power, and  $\sigma^2 = \frac{1}{M-K} \text{tr}\{\Lambda_n\}$ .

To minimize the value of the function  $\mathcal{F}(b)$ , we use the following two steps [31] :

*Step 1:* With the norm constraint  $\|b\|^2 = 1$ , obtain a  $b_1$  through minimizing the following function  $\mathcal{F}_1(b)$ :

$$\mathcal{F}_1(b) = \text{tr}\{B^H U_s W U_s^H B\} \quad (24)$$

*Step 2:* With the norm constraint  $\|b_1\|^2 = 1$ , obtain a  $b_2$  through minimizing the following function  $\mathcal{F}_2(b_1)$ :

$$\mathcal{F}_2(b_1) = \text{tr}\{(\hat{B}^H \hat{B})^{-1} B^H U_s W U_s^H B\} \quad (25)$$

where  $\hat{B}$  is made from the estimate  $b_1$  obtained in step 1, suppose  $|\hat{B}^H \hat{B}| \neq 0$ ,  $|\cdot|$  is the determinant of a matrix.

The angles of arrival are estimated through rooting the polynomial with coefficients  $b_2$ . Note that step 2 may be iterated for a few times [24].

## B. PDOA MEASUREMENT

Use  $d$  to represent the distance between a UHF RFID reader and a tag.  $\Delta t$  is the time that a signal needs to propagate from the reader to the tag and then return to the reader:

$$d = \frac{1}{2} c \Delta t \quad (26)$$

$$\phi = 2\pi f \Delta t \quad (27)$$

where  $c = 3 \times 10^8 \text{ m/s}$ ,  $f$  is the frequency of the signal,  $\phi$  is the phase delay of the signal after the time  $\Delta t$ .

From formula (26) and (27) we can get:

$$d = c \frac{\phi}{4\pi f} \quad (28)$$

If  $\phi = 2n\pi + \phi'$ :

$$d = \frac{1}{2} \lambda (n + \frac{\phi'}{2\pi}) \quad (29)$$

where  $n \in \mathbb{N}$ ,  $\lambda$  is the wavelength of the signal.

Through formula (29) we cannot get an accurate value of distance  $d$  because there is a  $2n\pi$  phase ambiguity. Therefore, we use two signals with different frequency  $f_1$  and  $f_2$ :

$$\phi_1 = 2n_1\pi + \phi'_1 = \frac{4\pi d f_1}{c} \quad (30)$$

$$\phi_2 = 2n_2\pi + \phi'_2 = \frac{4\pi d f_2}{c} \quad (31)$$

We assume that  $n_1 = n_2$ , it means that  $\phi_1$  and  $\phi_2$  have the same integral period.

Suppose  $f_2 > f_1$  and subtract formula (30) from (31):

$$\begin{cases} d = \frac{c \Delta \phi}{4\pi \Delta f}, & \text{if } \phi_2 > \phi_1 \\ d = \frac{c(\Delta \phi + 2\pi)}{4\pi \Delta f}, & \text{if } \phi_2 < \phi_1 \end{cases} \quad (32)$$

where  $\Delta \phi = \phi'_2 - \phi'_1$ ,  $\Delta f = f_2 - f_1$ .



When a signal meets an obstacle and it is reflected, there are reflection coefficients [17]:

$$R_{\perp} = \frac{\cos(\theta) - \sqrt{\varepsilon - \sin^2(\theta)}}{\cos(\theta) + \sqrt{\varepsilon - \sin^2(\theta)}} \quad (33)$$

$$R_{\parallel} = \frac{\varepsilon \cos(\theta) - \sqrt{\varepsilon - \sin^2(\theta)}}{\varepsilon \cos(\theta) + \sqrt{\varepsilon - \sin^2(\theta)}} \quad (34)$$

$$\varepsilon = \varepsilon_r - j60\sigma\lambda \quad (35)$$

where  $R_{\perp}$  is the vertical polarization reflection coefficient,  $R_{\parallel}$  is the horizontal polarization reflection coefficient,  $\theta$  is the angle of incidence,  $\varepsilon_r$  is the normalized relative dielectric constant of the reflecting surface,  $\sigma$  is the conductivity of the reflecting surface, and  $\lambda$  is the wavelength of the incident ray.

Through formula (33) and formula (34), we find there are phase changes in reflection coefficients. Suppose these phase changes are  $\phi_1''$  and  $\phi_2''$  for  $f_1$  and  $f_2$  respectively. These phase changes will affect the accuracy of the PDOA measurement.

However, from Fig. 2, we find that when the frequency difference  $\Delta f = f_2 - f_1$  is 5MHz, the phase change differences of the reflection coefficient  $\phi_2'' - \phi_1''$  are only about  $1 \times 10^{-4} \text{rad}$  and  $2 \times 10^{-4} \text{rad}$  respectively. Compared with  $\Delta\phi$ ,  $\phi_1'' - \phi_2''$  is very small.

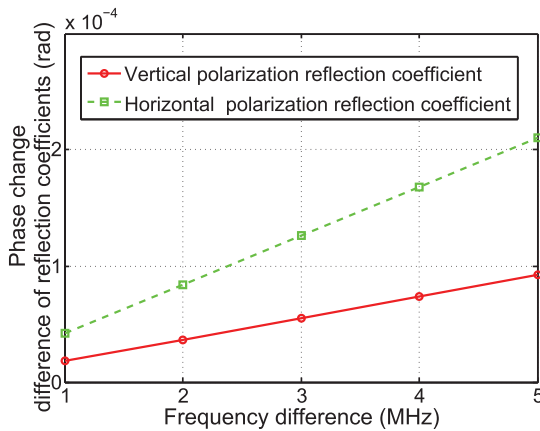


FIGURE 2. Phase changes difference of reflection coefficients for  $\theta = 45^\circ$ ,  $\varepsilon_r = 15$  and  $\sigma = 1$ .

In this paper, the maximum value of  $\Delta f$  is 5MHz, so we can neglect  $\phi_1'' - \phi_2''$ :

$$\begin{cases} d = \frac{c[\Delta\phi + (\phi_2'' - \phi_1'')]}{4\pi\Delta f} \approx \frac{c\Delta\phi}{4\pi\Delta f} & \text{if } \phi_2 > \phi_1 \\ d = \frac{c[\Delta\phi + 2\pi + (\phi_2'' - \phi_1'')]}{4\pi\Delta f} \\ \approx \frac{c(\Delta\phi + 2\pi)}{4\pi\Delta f} & \text{if } \phi_2 < \phi_1 \end{cases} \quad (36)$$

where  $\Delta f = f_2 - f_1$ , in two-dimensional environment,  $\phi_1'' = \arctan[\frac{\text{Im}(R_{\perp 1})}{\text{Re}(R_{\perp 1})}]$ ,  $\phi_2'' = \arctan[\frac{\text{Im}(R_{\perp 2})}{\text{Re}(R_{\perp 2})}]$ ,  $\text{Im}\{\cdot\}$  and  $\text{Re}\{\cdot\}$  are real part and imaginary part of a complex number respectively.

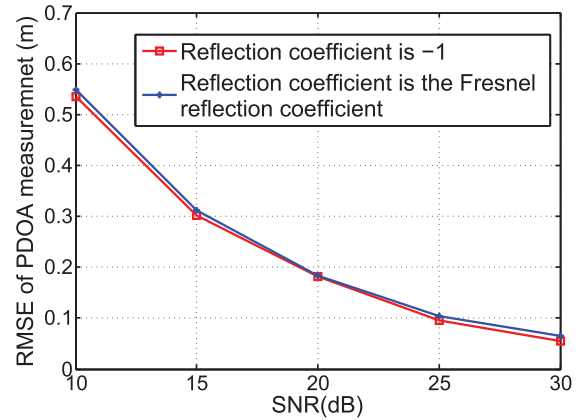


FIGURE 3. The comparison between PDOA measurement with reflection coefficient equal to -1 and Fresnel reflection coefficient,  $\Delta f = 5\text{MHz}$ .

From Fig. 3, we can observe that when reflection coefficient is Fresnel reflection coefficient, the RMSE of PDOA measurement is nearly the same with reflection coefficient equal to -1. It is consistent with our approximation in formula (36).

The maximum acceptable range of PDOA measurement is:

$$R_{max} = \frac{c}{2\Delta f} \quad (37)$$

where  $\Delta f = f_2 - f_1$ ,  $c = 3 \times 10^8 \text{m/s}$ .

### C. THE ESTABLISHMENT OF VIRTUAL STATION

In a real-world scenario, the wireless signal propagation has many complicated phenomena, such as NLOS, multipath, scatter, etc. In this paper, we only consider direct paths and reflection paths, and we neglect penetration paths and diffraction paths.

For direct paths, there is no need to establish virtual stations. We use  $X_t = [x_t, y_t]^T$  to represent localization of the tag, and use  $X_b = [x_b, y_b]^T$  to represent localization of the BS.  $d$  is the distance from  $X_t$  to  $X_b$  and  $\theta$  is the incidence angle,  $\theta \in [0, \pi]$ . The relationship between  $X_t$  and  $X_b$  is shown in formula (38):

$$X_t = X_b + [d \cos(\theta), d \sin(\theta)]^T \quad (38)$$

For reflection paths, firstly, we consider one-round reflection paths to explain how to establish virtual stations. As shown in Fig. 4, a straight line  $l$  is the reflector,  $X_b$  is the location of BS and  $X_v = [x_v, y_v]^T$  is the location of the virtual station. The broken line with arrow is the signal propagation path.  $\theta$  is the angle of incidence,  $\psi$  is the angle between positive  $x$  axis and  $l$ ,  $\theta'$  is the angle between positive  $x$  axis and the path from  $X_t$  to  $X_v$ ,  $\theta' \in [-\pi, \pi]$ .  $\alpha$  and  $\beta$  are the angles between positive  $x$  axis and the lines from  $X_v$  to the ends of the straight line  $l$ ,  $\alpha < \beta$ .

Let  $Ax + By + C = 0$  represent  $l$ , the distance between  $X_b$  and  $l$  is:

$$d' = |Ax_b + By_b + C| / \sqrt{A^2 + B^2} \quad (39)$$

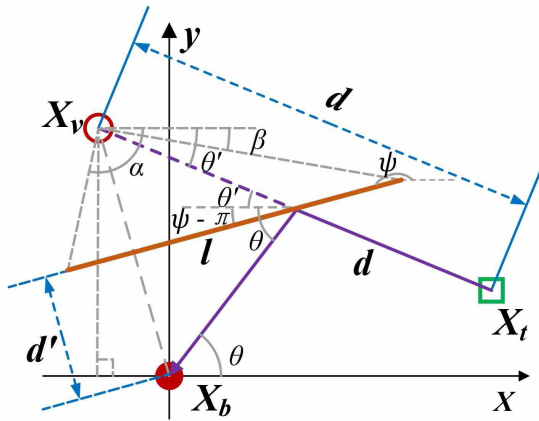


FIGURE 4. Establishment of virtual stations based on one-round reflection paths.

The location of  $X_v$  is:

$$X_v = X_b + P \quad (40)$$

where  $P = 2d'[\cos(\psi - \pi/2), \sin(\psi - \pi/2)]^T$ , when  $X_b$  is below or on the left of  $l$ ;  $P = -2d'[\cos(\psi - \pi/2), \sin(\psi - \pi/2)]^T$ , when  $X_b$  is above or on the right of  $l$ ,  $\psi$  is the angle between positive  $x$  axis and  $l$ .

After we know the position of  $X_v$ , we can obtain the location of  $X_t$ :

$$X_t = X_v + Q \quad (41)$$

where  $Q = [d \cos(\theta'), d \sin(\theta')]^T$ .  $\theta'$  is the angle between positive  $x$  axis and the path from  $X_t$  to  $X_v$ ,  $\theta' \in [-\pi, \pi]$ .

From the geometric relationship, we can derive:

$$|\theta'| = \theta - 2\psi \quad (42)$$

Now we analyse that under what condition reflections can happen. Firstly, the distance measured by PDOA should be larger than the distance between BS and the reflector; Secondly, the reflection point should be on the reflector.

$$\begin{cases} d > d' \\ \theta' \in (\alpha, \beta) \end{cases} \quad (43)$$

where  $\alpha$  and  $\beta$  are the angles between positive  $x$  axis and the lines from  $X_v$  to the ends of the straight line  $l$ ,  $\alpha < \beta$ .

For multiple-rounds reflection paths, as shown in Fig. 5, there are  $n$  reflectors and we use straight lines  $l_i$  to represent them (to show the figure clearly, we only draw two reflectors).  $X_b$  and  $X_{v0}$  are the position of the real station. The broken line with arrow is the signal propagation path.  $\theta_0$  is the angle of incidence.  $X_{t3}$  is the position of RFID tag to be positioned.  $X_{t1}$  and  $X_{t1}$  are the positions derived from the real station  $X_b$  and the virtual station  $X_{v1}$ .  $\theta_j$  is the angle between positive  $x$  axis and the path from  $X_{tj}$  to  $X_{v(j-1)}$ ,  $\alpha_i$  and  $\beta_i$  are the angles between positive  $x$  axis and the lines from  $X_{vi}$  to the ends of the straight line  $l_i$  respectively,  $\alpha_i < \beta_i$ .

$$A_i x + B_i y + C_i = 0, \quad i = 1, 2, \dots, n. \quad (44)$$

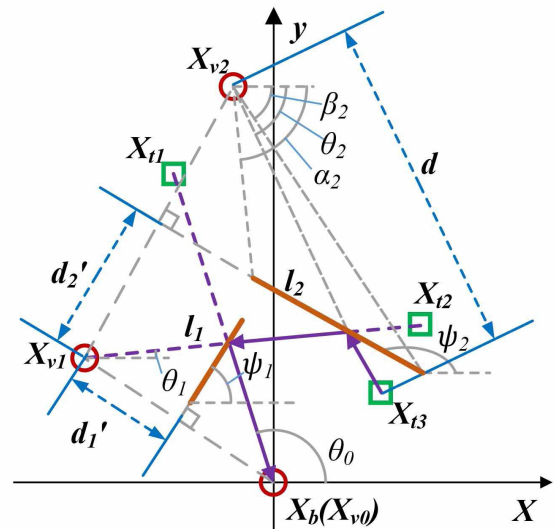


FIGURE 5. Establishment of virtual stations based on multiple-rounds reflection paths.

For every reflector, there should be a virtual station  $X_{vi}$ :

$$X_{vi} = X_{v(i-1)} + P_i, \quad i = 1, 2, \dots, n. \quad (45)$$

where  $P_i = 2d'_i[\cos(\psi_i - \pi/2), \sin(\psi_i - \pi/2)]^T$ , when  $X_{v(i-1)}$  is below or on the left of  $l_i$ ;  $P_i = -2d'_i[\cos(\psi_i - \pi/2), \sin(\psi_i - \pi/2)]^T$ , when  $X_{v(i-1)}$  is above or on the right of  $l_i$ ,  $\psi_i$  is the angle between positive  $x$  axis and  $l_i$ ,  $X_{v0}$  is equal to  $X_b = [x_b, y_b]^T$ ,

$$d'_i = \frac{|A_i x_{v(i-1)} + B_i y_{v(i-1)} + C_i|}{\sqrt{A_i^2 + B_i^2}} \quad (46)$$

The possible positions of tag can be expressed as follows:

$$X_{tj} = X_{v(j-1)} + Q_{j-1}, \quad j = 1, 2, \dots \quad (47)$$

where  $Q_{j-1} = [d \cos(\theta_{j-1}), d \sin(\theta_{j-1})]^T$ ,  $\theta_j$  is the angle between positive  $x$  axis and the path from  $X_{tj}$  to  $X_{v(j-1)}$ ,  $|\theta_j| = \theta_{(j-1)} - 2\psi_j$ .

We should analyse every reflector from  $i = 1$  to  $i = n$ , and we can stop when  $i = n$  or  $d < d'_i$  or  $\theta_i \notin (\alpha_i, \beta_i)$ ,  $\alpha_i$  and  $\beta_i$  are the angles between positive  $x$  axis and the lines from  $X_{vi}$  to the ends of the straight line  $l_i$  respectively,  $\alpha_i < \beta_i$ .

#### IV. LOCATION ESTIMATION ALGORITHM AND THE CRLB

##### A. LOCATION ESTIMATION ALGORITHM

Based on a pair of distance  $d$  and angle  $\theta$ , we can obtain more than one possible positions of the tag by using virtual stations. Therefore, we need at least two pairs of  $d$  and  $\theta$  to find the real position of the tag.

Let  $X_{1ti} = [x_{1ti}, y_{1ti}]^T$  and  $X_{2tj} = [x_{2ti}, y_{2ti}]^T$  be the possible positions of the tag which are derived from the first and second signal paths respectively,  $i = 1, 2, \dots, n_1$ ,  $j = 1, 2, \dots, n_2$ .

If the values of  $d$  and  $\theta$  have no error, there must exist  $i$  and  $j$  that can make  $X_{1ti} = X_{2tj}$ , and it is the exact position of the tag. However, noise, multiple paths propagation and

other effects make the estimation of  $d$  and  $\theta$  not very exact, so we try to find a pair of  $X_{1ti}$  and  $X_{2tj}$  which have the shortest distance:

$$[I, J] = \arg \min_{i \in [1, n_1], j \in [1, n_2]} f(i, j) \quad (48)$$

where

$$f(i, j) = \sqrt{(x_{1ti} - x_{2tj})^2 + (y_{1ti} - y_{2tj})^2} \quad (49)$$

According to the formula (47), if we know the location of  $X_{1tI}$  and  $X_{2tJ}$ , we can calculate  $X_{1v(I-1)}$  and  $X_{2v(J-1)}$ .

Suppose there are  $N$  pairs of  $d$  and  $\theta$  which are estimated by the base station,  $X_k = [x_k, y_k]^T$ ,  $k = 1, 2, \dots, N$  is the virtual stations corresponding to the positions of the tag which are derived from the  $k$ th signal path;  $d_k$  is the length of the  $k$ th signal path which is measured by PDOA estimation and  $d_k < d_{k+1}$ ;  $\theta_k$  is the angle which is derived from the AOA estimation. Use  $X = [x, y]^T$  to represent the location of the tag to be calculated:

$$-2x_i x - 2y_i y + x^2 + y^2 = d_i^2 - x_i^2 - y_i^2 \quad (50)$$

$$x \sin(\theta_i) - y \cos(\theta_i) = x_i \sin(\theta_i) + y_i \cos(\theta_i) \quad (51)$$

Use matrixs to represent formula (50) and (51):

$$GZ = H \quad (52)$$

where

$$G = \begin{bmatrix} -2x_1 & -2y_1 & 1 \\ \vdots & \vdots & \vdots \\ -2x_N & -2y_N & 1 \\ \sin(\theta_1) & \cos(\theta_1) & 0 \\ \vdots & \vdots & \vdots \\ \sin(\theta_N) & \cos(\theta_N) & 0 \end{bmatrix} \quad (53)$$

$$H = \begin{bmatrix} d_1^2 - (x_1^2 + y_1^2) \\ \vdots \\ d_N^2 - (x_N^2 + y_N^2) \\ x_1 \sin(\theta_1) - y_1 \cos(\theta_1) \\ \vdots \\ x_N \sin(\theta_N) - y_N \cos(\theta_N) \end{bmatrix} \quad (54)$$

$$Z = [x, y, x^2 + y^2]^T \quad (55)$$

Now we use weighted least squares combined with residual weighted (WLS-RW) algorithm to find the value of  $x$  and  $y$ .

$$Z_1 = [x', y', x'^2 + y'^2]^T = (G^T W G)^{-1} G^T W H \quad (56)$$

where  $W = \frac{1}{B} \text{diag}\{d_N^2, \dots, d_1^2, d_N^2, \dots, d_1^2, \}$ ,  $B = \sum_{i=1}^N d_i^2$ , suppose  $|G^T W G| \neq 0$ ,  $|\cdot|$  is the determinant of a matrix.

We can get the position of the tag  $X = [x, y]^T$  through residual weighted algorithm:

$$x = \frac{(d_{wN} - d_N)^2 x'_1 + \dots + (d_{w1} - d_1)^2 x'_N}{(d_{wN} - d_N)^2 + \dots + (d_{w1} - d_1)^2} \quad (57)$$

$$y = \frac{(d_{wN} - d_N)^2 y'_1 + \dots + (d_{w1} - d_1)^2 y'_N}{(d_{wN} - d_N)^2 + \dots + (d_{w1} - d_1)^2} \quad (58)$$

where

$$d_{wk} = \sqrt{(x' - x_k)^2 + (y' - y_k)^2} \quad k = 1, 2, \dots, N. \quad (59)$$

$X'_i = [x'_i, y'_i]^T$   $i = 1, 2, \dots, N$  is the position of the tag derived from the  $i$ th signal path, which can be calculated through the formula (47) and (48).

## B. THE CRAMÉR-RAO LOWER BOUNDS

In AOA estimation, consider the number of the sampling snapshot is  $K$  and the number of array elements is  $M$ , from formula (8), we derive the probability density function:

$$\mathcal{P} = |\pi \sigma^2 I_M|^{-K} e^{(-\sigma^{-2} \sum_{t=1}^K \|X(t) - AS(t)\|_2^2)} \quad (60)$$

where  $\sigma^2$  is the variance of the noise,  $I_M \in \mathbb{C}^{M \times M}$  is the identity matrix  $A = [a(\theta_1), \dots, a(\theta_K)]^T$ ,  $S(t) = [s_1(t), \dots, s_K(t)]^T$ .

The log-likelihood function is:

$$\mathcal{L} = -MKL n \sigma^2 - \sigma^2 \sum_{t=1}^K \|X(t) - AS(t)\|_2^2 \quad (61)$$

Suppose  $|A^H A| \neq 0$ ,  $|\cdot|$  is the determinant of a matrix, from formula (61), we can derive the CRLB of the AOA estimation:

$$\sigma_\theta = \frac{\sigma^2}{2} \left\{ \sum_{t=1}^K \text{Re}[A_t^H D^H P D A_t] \right\}^{-1/2} \quad (62)$$

where

$$A_t = \text{diag}\{[s_1(t), s_2(t), \dots, s_K(t)]^T\} \quad (63)$$

$$D = [d(\theta_1), \dots, d(\theta_K)] \quad (64)$$

$$d(\theta) = da(\theta)/d\theta \quad (65)$$

$$P = I_M - (A^H A)^{-1} A^H \quad (66)$$

The CRLB of the PDOA estimation is [28]:

$$\sigma_d = \frac{c}{2} \sqrt{\frac{1}{8\pi^2 (f_1^2 + \frac{W^2}{4}) \text{snr} W T_0}} \quad (67)$$

where  $c = 3 \times 10^8 \text{m/s}$ ,  $W = f_2 - f_1$ ,  $f_2 > f_1$ ,  $T_0$  is the duration of time for observing the signal.

Calculate the position of the tag  $X = [x, y]^T$  through WLS-RW with  $d_i = d_{si} + \sigma_{di}$  and  $\theta_i = \theta_{si} + \sigma_{\theta i}$ ,  $i = 1, 2, \dots, N$ , CRLB of the the localization error is:

$$\sigma_{loc} = \sqrt{(x - x_r)^2 + (y - y_r)^2} \quad (68)$$

where  $d_{si}$  and  $\theta_{si}$  are the distance and angle value obtained from the ray-tracing,  $X_r = [x_r, y_r]$  is the real position of the tag.

## V. SIMULATION AND RESULTS

We use Matlab to simulate the proposed method. Fig. 6 shows the simulation environment. We use a 10m\*10m room to establish our simulation environment, there are two reflectors in the room. The ULA contains 10 array elements and we use a small circle to represent each of them. To show the signal

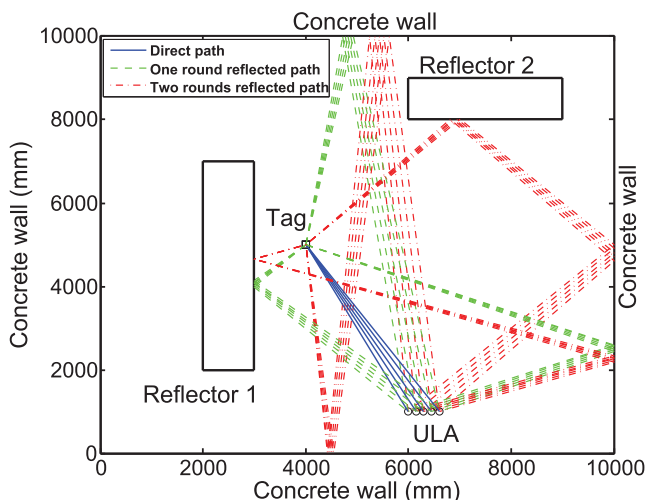


FIGURE 6. A Simulation environment of indoor localization using AOA and PDOA based on passive UHF RFID.

paths clearly we only draw 5 small array elements in the figure. The small rectangle represents a tag to be positioned. The ULA can only receive the signals with directions from  $0^\circ$  to  $180^\circ$  and the main beamwidth is about  $10^\circ$ . We use the ray-tracing to simulate the signal propagation paths. From the figure, we can see that there are one direct path from the tag to reader, three one-round reflected paths and three two-rounds reflected path. Algorithm 1 shows the steps of our proposed method.

**Algorithm 1** Indoor Localization With AOA + PDOA + Virtual Stations

- 1: Distinguish the multipath signals with array antenna.
- 2: Choose two strongest paths according to RSS.
- 3: Obtain phase information of the two paths from the ULA.
- 4: Get  $\mathbf{H}$  and estimate the angles with MODE algorithm.
- 5: Estimate the distances through PDOA method.
- 6: Establish virtual stations according to the location of the BS and obstacles.
- 7: Calculate possible positions  $X_{1ti}$  and  $X_{2tj}$  of the tag.
- 8: Find  $X_{1tI}$  and  $X_{2tJ}$ , and calculate  $X_{1v(I-1)}$  and  $X_{2v(J-1)}$ .
- 9: Calculate the location of the tag with WLS-RW algorithm.

**A. ERROR OF LOCALIZATION**

Fig. 7 shows the RMSE of localization versus SNR with LS, WLS, LS-RW, WLS-RW algorithms and CRLB. We can observe that, with WLS-RW algorithm, when SNR is larger than 10dB, the RMSE is smaller than 0.6m, and when the SNR is larger than 15dB, the RMSE is smaller than 0.2m. Fig. 8 shows the cumulative distribution function (CDF) of localization error. Fig. 9 shows the RMSE of localization error versus SNR for two signal paths with different RSS, we can observe that the localization error has the smallest value when the two signal paths have the strongest RSS. Fig. 10 is the CDF of localization error when array

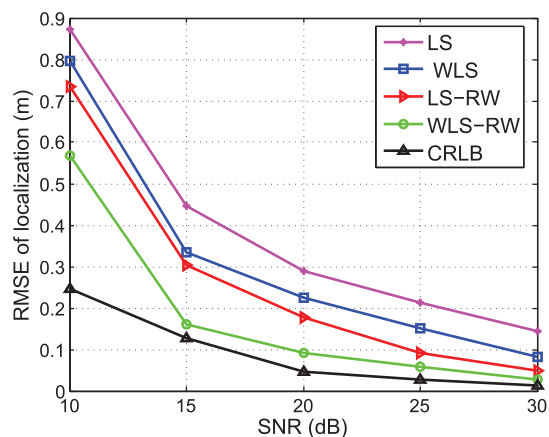


FIGURE 7. The RMSE of localization versus SNR with LS, WLS, LS-RW, WLS-RW algorithm and CRLB, the number of array element is 10, the result is obtained through 500 Monte Carlo simulations.

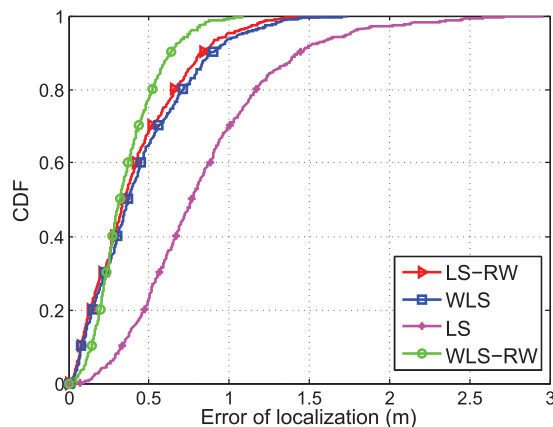


FIGURE 8. CDF of localization error, SNR=10dB, the result is obtained through 500 Monte Carlo simulations.

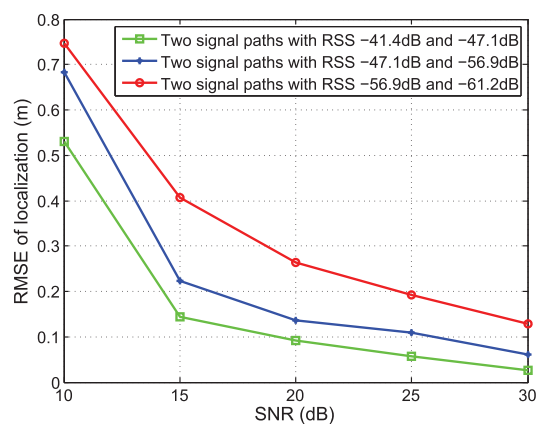


FIGURE 9. The RMSE of localization error versus SNR, with WLS-RW algorithm, for two signal paths with different RSS.

element is 6, 9, 16. Beamwidth is calculated through equation (14). From this figure we can easily observe that when the beamwidth is narrower, the accuracy of localization is higher.

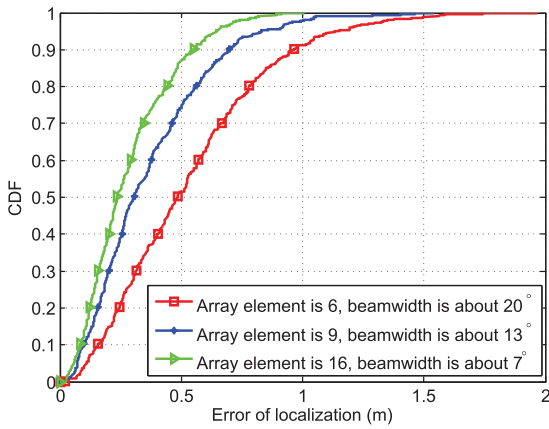


FIGURE 10. CDF of localization error, with WLS-RW algorithm, when beamwidth of the array antenna is about 20°, 13°, 7°, SNR=10dB, the result is obtained through 500 Monte Carlo simulations.

B. PDOA ESTIMATION

Fig. 11 shows the CDF of distance error measured by PDOA with the frequency difference  $\Delta f=1,5,10$  and 15MHz, it can be observed that the distance error of large frequency difference is less than the distance error of small frequency difference.

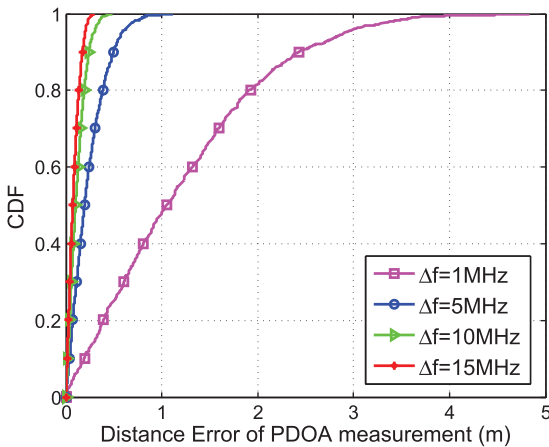


FIGURE 11. CDF of distance error with PDOA measurement, SNR=20dB, the result is obtained through 1000 Monte Carlo simulations.

However, from Fig. 12, we can observe, as the frequency difference increases, the acceptable measuring distance decreases, so in general case, we let  $\Delta f$  equal to 5MHz to ensure the accuracy and the acceptable range of PDOA measurement.

C. AOA ESTIMATION

The comparison between MUSIC with spatial smoothing and MODE algorithm is shown in Fig. 13. In the simulation, we use a ULA with inter-element spacing 0.15m, and the sampling number is 512. 100 times Monte Carlo simulations are carried out. From the result, we can observe that the MODE has a better performance than MUSIC algorithm with spatial smoothing.

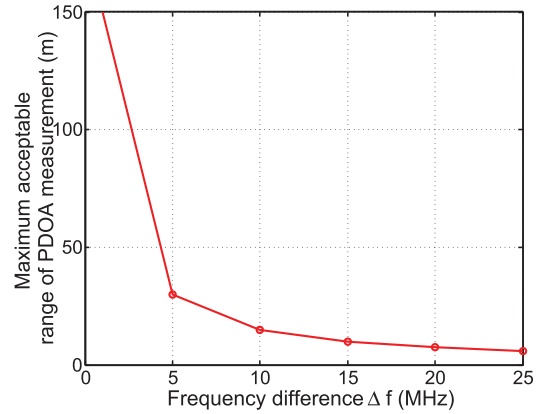


FIGURE 12. Maximum acceptable range of PDOA measurement versus frequency difference.

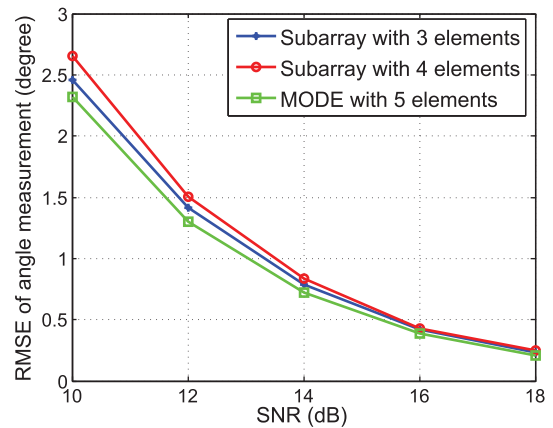


FIGURE 13. The comparison between MUSIC with spatial smoothing and MODE, the number of array element is 5.

VI. CONCLUSION

UHF RFID positioning technique is more and more popular in localization methods. In this paper, we propose an indoor localization method based on AOA and PDOA using virtual stations for passive UHF RFID in multipath and NLOS environments. The array antenna with narrow beamwidth is used to distinguish the multipath signals, and virtual stations are established to convert the NLOS paths into LOS paths. Both the AOA and PDOA information are used to locate the tag with WLS-RW algorithm. Based on the simulation results, our proposed method can achieve decimeter level accuracy and has higher precision than some traditional algorithms. For the future work, we will continue to study hybrid UHF RFID localization methods to improve the accuracy and efficiency of indoor positioning systems.

REFERENCES

[1] Q. Jiang, Y. Ma, K. Liu, and Z. Dou, "A probabilistic radio map construction scheme for crowdsourcing-based fingerprinting localization," *IEEE Sensors J.*, vol. 16, no. 10, pp. 3764–3774, May 2016.  
 [2] S. Sourour, Y. Lohan, S. Valaee, and K. Majeed, "Joint indoor localization and radio map construction with limited deployment load," *IEEE Trans. Mobile Comput.*, vol. 14, no. 5, pp. 1031–1043, May 2015.



- [3] Y. Geng and K. Pahlavan, "Design, implementation, and fundamental limits of image and RF based wireless capsule endoscopy hybrid localization," *IEEE Trans. Mobile Comput.*, vol. 15, no. 8, pp. 1951–1964, Aug. 2016.
- [4] J. He, Y. Geng, and K. Pahlavan, "Toward accurate human tracking: Modeling time-of-arrival for wireless wearable sensors in multipath environment," *IEEE Sensors J.*, vol. 14, no. 11, pp. 3996–4006, Nov. 2014.
- [5] A. Makki, A. Siddig, M. Saad, J. R. Cavallaro, and C. J. Bleakley, "Indoor localization using 802.11 time differences of arrival," *IEEE Trans. Instrum. Meas.*, vol. 65, no. 3, pp. 614–623, Mar. 2016.
- [6] C.-C. Huang and H.-N. Manh, "RSS-based indoor positioning based on multi-dimensional kernel modeling and weighted average tracking," *IEEE Sensors J.*, vol. 16, no. 9, pp. 3231–3245, May 2016.
- [7] J. Zhou, H. Zhang, and L. Mo, "Two-dimension localization of passive RFID tags using AOA estimation," in *Proc. IEEE Instrum. Meas. Technol. Conf. (I2MTC)*, May 2011, pp. 1–5.
- [8] S. Azzouzi, M. Cremer, U. Dettmar, R. Kronberger, and T. Knie, "New measurement results for the localization of UHF RFID transponders using an angle of arrival (AoA) approach," in *Proc. IEEE Int. Conf. (RFID)*, Apr. 2011, pp. 91–97.
- [9] T. Chen, L. Liu, and D. Pan, "A ULA-based MWC discrete compressed sampling structure for carrier frequency and AOA estimation," *IEEE Access*, vol. 5, pp. 14154–14164, 2017.
- [10] J. Wang, Y. Ma, Y. Zhao, and K. Liu, "A multipath mitigation localization algorithm based on MDS for passive UHF RFID," *IEEE Commun. Lett.*, vol. 19, no. 9, pp. 1652–1655, Sep. 2015.
- [11] A. Naz, H. M. Asif, T. Umer, and B.-S. Kim, "PDOA based indoor positioning using visible light communication," *IEEE Access*, vol. 6, pp. 7557–7564, 2018.
- [12] Y. Ma, L. Zhou, K. Liu, and J. Wang, "Iterative phase reconstruction and weighted localization algorithm for indoor RFID-based localization in NLOS environment," *IEEE Sensors J.*, vol. 14, no. 2, pp. 597–611, Feb. 2014.
- [13] S. Azzouzi, M. Cremer, U. Dettmar, T. Knie, and R. Kronberger, "Improved AoA based localization of UHF RFID tags using spatial diversity," in *Proc. IEEE Int. Conf. RFID-Technol. Appl. (RFID-TA)*, Sep. 2011, pp. 174–180.
- [14] P. Yang, W. Wu, M. Moniri, and C. C. Chibelushi, "Efficient object localization using sparsely distributed passive RFID tags," *IEEE Trans. Ind. Electron.*, vol. 60, no. 12, pp. 5914–5924, Dec. 2013.
- [15] K. Yu and E. Dutkiewicz, "Improved Kalman filtering algorithms for mobile tracking in NLOS scenarios," in *Proc. IEEE Wireless Commun. Netw. Conf. (WCNC)*, Apr. 2012, pp. 2390–2394.
- [16] T. Liu, Y. Liu, L. Yang, Y. Guo, and C. Wang, "BackPos: High accuracy backscatter positioning system," *IEEE Trans. Mobile Comput.*, vol. 15, no. 3, pp. 586–598, Mar. 2016.
- [17] D. Liu, M.-C. Lee, C.-M. Pun, and H. Liu, "Analysis of wireless localization in nonlinear-of-sight conditions," *IEEE Trans. Veh. Technol.*, vol. 62, no. 4, pp. 1484–1492, May 2013.
- [18] Y. Zhao, N. Patwari, P. Agrawal, and M. Rabbat, "Directed by directionality: Benefiting from the gain pattern of active RFID badges," *IEEE Trans. Mobile Comput.*, vol. 11, no. 5, pp. 865–877, May 2012.
- [19] M. R. Basheer and S. Jagannathan, "Localization of RFID tags using stochastic tunneling," *IEEE Trans. Mobile Comput.*, vol. 12, no. 6, pp. 1225–1235, Jun. 2013.
- [20] Z. Zhang, Z. Lu, V. Saakian, X. Qin, Q. Chen, and L.-R. Zheng, "Item-level indoor localization with passive UHF RFID based on tag interaction analysis," *IEEE Trans. Ind. Electron.*, vol. 61, no. 4, pp. 2122–2135, Apr. 2014.
- [21] A. Badawy, T. Khattab, D. Trincherro, T. M. Elfouly, and A. Mohamed, "A simple cross correlation switched beam system (XSBS) for angle of arrival estimation," *IEEE Access*, vol. 5, pp. 3340–3352, 2017.
- [22] B. R. Jackson, S. Rajan, B. J. Liao, and S. Wang, "Direction of arrival estimation using directive antennas in uniform circular arrays," *IEEE Trans. Antennas Propag.*, vol. 63, no. 2, pp. 736–747, Feb. 2015.
- [23] M. L. Bencheikh and Y. Wang, "Joint DOD-DOA estimation using combined ESPRIT-MUSIC approach in MIMO radar," *Electron. Lett.*, vol. 46, no. 15, pp. 1081–1083, Jul. 2010.
- [24] P. Stoica and K. Sharman, "Maximum likelihood methods for direction-of-arrival estimation," *IEEE Trans. Acoust., Speech Signal Process.*, vol. 38, no. 7, pp. 1132–1143, Jul. 1990.
- [25] D. Liu, K. Liu, Y. Ma, and J. Yu, "Joint TOA and DOA localization in indoor environment using virtual stations," *IEEE Commun. Lett.*, vol. 18, no. 8, pp. 1423–1426, Aug. 2014.
- [26] Z.-M. Liu, "Conditional Cramér–Rao lower bounds for doa estimation and array calibration," *IEEE Signal Process. Lett.*, vol. 21, no. 3, pp. 361–364, Mar. 2014.
- [27] I. Kazemi, M. R. Moniri, and R. S. Kandovan, "Optimization of angle-of-arrival estimation via real-valued sparse representation with circular array radar," *IEEE Access*, vol. 1, pp. 404–407, 2013.
- [28] Y. Ma, K. Pahlavan, and Y. Geng, "Comparison of POA and TOA based ranging behavior for RFID application," in *Proc. IEEE 25th Annu. Int. Symp. Pers., Indoor, Mobile Radio Commun. (PIMRC)*, Sep. 2014, pp. 1722–1726.
- [29] H. T. Friis, "A note on a simple transmission formula," *Proc. IRE*, vol. 34, no. 5, pp. 254–256, May 1946.
- [30] P. V. Nikitin, K. V. S. Rao, S. F. Lam, V. Pillai, R. Martinez, and H. Heinrich, "Power reflection coefficient analysis for complex impedances in RFID tag design," *IEEE Trans. Microw. Theory Techn.*, vol. 53, no. 9, pp. 2721–2725, Sep. 2005.
- [31] F. Wen and C. Liang, "Fine-grained indoor localization using single access point with multiple antennas," *IEEE Sensors J.*, vol. 15, no. 3, pp. 1538–1544, Mar. 2015.
- [32] A. B. Gershman and P. Stoica, "MODE with extra-roots (MODEX): A new DOA estimation algorithm with an improved threshold performance," in *Proc. IEEE Int. Conf. Acoust., Speech, Signal Process. (ICASSP)*, vol. 5, Mar. 1999, pp. 2833–2836.



**YONGTAO MA** (M'12) was born in Weifang, China. He received the B.S. degree in electronic information engineering and the M.S. and Ph.D. degrees in circuits and systems from Tianjin University, Tianjin, China, in 2001, 2005, and 2009, respectively. He is currently an Associate Professor with the School of Microelectronics, Tianjin University. His current research interests include wireless localization, radio frequency identification, cognitive radio, and microwave technology.



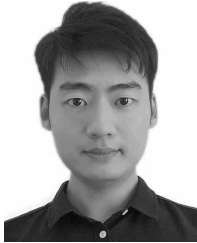
**BOBO WANG** received the B.E. degree from the School of Electrical and Information Engineering from the Jiangsu University of Technology, Changzhou, China, in 2013, and the M.E. degree from the College of Electronic Information and Automation, Civil Aviation University of China, Tianjin, China, in 2017. He is currently pursuing the Ph.D. degree with the School of Microelectronics, Tianjin University, China. His current research interests include radio frequency identification and indoor localization.



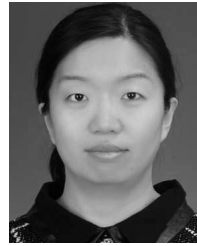
**SHUYANG PEI** was born in Chifeng, China, in 1993. She received the B.Eng. degree in integrated circuit design and integration system from Tianjin University, Tianjin, China, in 2015, and the M.S. degree from the School of Microelectronics, Tianjin University. Her current research interests include machine learning, radio frequency identification, and indoor localization.



**YUNLEI ZHANG** received the B.Eng. degree in electronic information engineering and the M.S. degree in electronic and communication engineering from Tianjin University, Tianjin, China, in 2014 and 2017, respectively, where he is currently pursuing the Ph.D. degree with the School of Microelectronics. His current research interests include indoor localization and massive MIMO.



**SHUAI ZHANG** received the B.S. degree in electronic information science and technology from Nankai University, Tianjin, China, in 2012, and the M.S. degree in information and communication engineering from the Tianjin University of Technology, Tianjin, in 2016, where he is currently pursuing the Ph.D. degree with the School of Microelectronics. His current research interests include machine learning and indoor localization.



**JIEXIAO YU** (M'15) was born in Tianjin, China. She received the B.S. degree in electronic information engineering from Nankai University in 2002 and the M.S. degree in theory and new technology of electrical engineering and the Ph.D. degree in circuits and systems from Tianjin University, Tianjin, in 2005 and 2009, respectively. She is currently an Associate Professor with the School of Electrical and Information Engineering, Tianjin University. Her current research interests include wireless localization, radio frequency identification, WSN, and array signal processing.

• • •